



**HAL**  
open science

# Anomalous fractional diffusion equation for magnetic losses in a ferromagnetic lamination

B. Ducharne, Y. Deffo, B. Zhang, G. Sebald

► **To cite this version:**

B. Ducharne, Y. Deffo, B. Zhang, G. Sebald. Anomalous fractional diffusion equation for magnetic losses in a ferromagnetic lamination. *The European Physical Journal Plus*, 2020, 135 (3), 10.1140/epjp/s13360-020-00330-x . hal-02559894

**HAL Id: hal-02559894**

**<https://hal.science/hal-02559894>**

Submitted on 11 Apr 2022

**HAL** is a multi-disciplinary open access archive for the deposit and dissemination of scientific research documents, whether they are published or not. The documents may come from teaching and research institutions in France or abroad, or from public or private research centers.

L'archive ouverte pluridisciplinaire **HAL**, est destinée au dépôt et à la diffusion de documents scientifiques de niveau recherche, publiés ou non, émanant des établissements d'enseignement et de recherche français ou étrangers, des laboratoires publics ou privés.

# Anomalous fractional diffusion equation for magnetic losses in a ferromagnetic lamination.

Ducharne B.<sup>1</sup>, Y.A. Tene Deffo<sup>1,2</sup>, B. Zhang<sup>3</sup>, G. Sebald<sup>4</sup>

<sup>1</sup>Laboratoire de Génie Electrique et Ferroélectricité – INSA de Lyon, Villeurbanne, France.

<sup>2</sup>Faculty of Engineering and Technology, University of Buea, Buea, Cameroon.

<sup>3</sup>Green Manufacturing R&D Laboratory, School of Mechanical, Electrical and Information Engineering, Shandong University, Weihai, China.

<sup>4</sup>ELyTMaX UMI 3757, CNRS – Université de Lyon – Tohoku University, International Joint Unit, Tohoku University, Sendai, Japan.

## **Abstract**

During a full magnetization cycle and under a collinearity situation, the magnetic losses in a ferromagnetic are observable by plotting the average magnetic flux density or magnetization as a function of the tangent magnetic excitation. This highly frequency dependent magnetic signature is called hysteresis cycle and its area is equal to the energy consumed during the magnetization cycle. The physical mechanisms behind this energy conversion are complex as they interfere and take place at different geometrical scales. Microscopic Eddy currents due to domain wall variations plays an important role, as well as the macroscopic Eddy currents due to the excitation field time variations and ruled by the magnetic field diffusion equation. From the literature on this topic, researchers have been proposing simulation models to reproduce and understand those complex observations. Even if all these losses contributions are physically interconnected, most of the simulation models available in the literature are based on the magnetic losses separation principle where each contribution is considered separately. Physically, the Weiss domains distribution and movements distort the diffusion process which becomes anomalous. In this article, the standard magnetic field diffusion equation is modified to take into account such anomaly. The first-order time derivation of the magnetic induction diffusion is replaced by a fractional order time derivation. This change offers flexibility in the simulation scheme as the fractional order can be considered as an additional degree of freedom. By adjusting precisely this order, very accurate simulation results can be obtained on a very broad frequency bandwidth for the prediction of the iron losses in a ferromagnetic material.

## **Keywords**

Anomalous diffusion, magnetic hysteresis, frequency dependence.

## I - Introduction

The magnetization processes in a ferromagnetic material are incredibly complex. Multiscale phenomena interfere, they depend highly on the surrounding conditions (temperature, pressure, geometry ...). Under the influence of an external magnetic excitation, the stability of the magnetic domains distribution is disturbed and movements, fusions, nucleation, spread all over the magnetic sample [1]. The magnetic losses due to the magnetization cycles in a ferromagnetic material are highly frequency  $f$  dependent [2]-[5]. They manifest themselves while plotting the evolution of the material magnetic state (the magnetic induction field  $B$ ) as a function of the external tangent magnetic excitation field  $H$ , the hysteresis cycle  $B(H)$ . The area of the hysteresis cycle is equal to the magnetic losses, i.e. the energy consumed during a magnetization cycle. It is admitted that below a given frequency known as the quasi-static threshold, the hysteresis cycle shape remains unchanged. Under such conditions, it is also admitted that the magnetic losses are mainly due to the microscopic Eddy currents induced around the moving domain walls or directly inside them. For higher frequencies, the frequency dependence is clearly noticeable as the hysteresis shape is strongly modified. As  $f$  increases and under "maximum  $H$ " imposed conditions, the hysteresis area increases first, then decreases gradually. A full decline can even be envisaged under extreme frequency levels. Under "maximum  $B$ " imposed conditions, the hysteresis cycle area increases continuously at a slow rate (see fig. 1). Beyond the quasi-static threshold, domain walls and microscopic Eddy currents are still acting but they interfere with macroscopic Eddy currents which origin is linked to the external magnetic excitation field  $H$  variations. Ferromagnetic hysteresis, frequency dependence, Eddy currents interactions ... have been studied for decades and a large number of simulation approaches can be found in the scientific literature [2]-[7]. The first experimental studies dealing with magnetic domains and wall distributions have been proposed by Bitter at the beginning of the 20<sup>th</sup> century [8]. A few years later, Weiss in [9][10] published his theoretical hypothesis leading towards the idea of magnetic domains in ferromagnetic materials. Right after, Pry & Bean in [11] confirmed the idea of magnetic domains, and established the first connection between their movements and some potential magnetic losses due to the

magnetization cycle. But Steinmetz was the first one to propose an empirical loss power law ( $B$  and  $f$  dependent) to theoretically consider the magnetic losses in a ferromagnetic lamination [12]. Later again, Bertotti et al. in a large number of publications proposed the well-known losses separation principle which is still today probably the most standard approach used to consider magnetic losses inside an electromagnetic device [13][14]. According to Bertotti, the magnetic losses in a ferromagnetic lamination can be separated into three contributions: The frequency independent quasi-static hysteresis losses, the first order  $f^1$  frequency dependent standard losses and the square root  $f^{0.5}$  frequency dependent excess losses. Fig. 1 below gives an illustration of the losses separation principle:

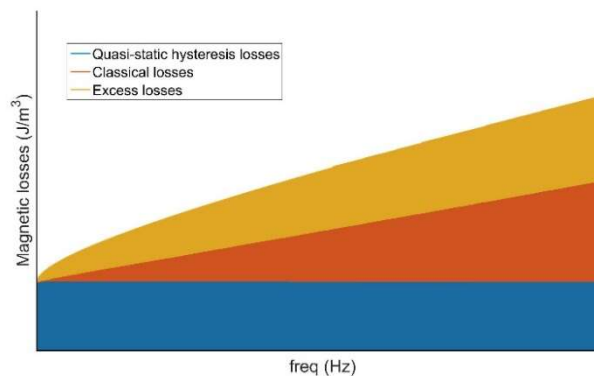


Fig. 1 – Illustration of the magnetic separation losses principle as proposed by Bertotti.

Even if this approach gives accurate results, it is still limited to given conditions and hypotheses, and it considers only harmonic excitation, making it inappropriate to time dependent simulations. The idea of separate contributions is furthermore contradictory with the physical nature of the magnetization processes where multiscale behavior interactions are dominant. Even rarely described, simultaneous resolutions are somehow possible, in [2] Raulet & al. proposed as an example a modified dynamic field diffusion equation. This strong formulation solves, in a simultaneous way, the diffusion equation and a dynamic material law. Space discretized finite differences are used to solve the diffusion equation. For every nodes, locals  $B$  and  $H$  are connected through the dynamic material law. This law is made out of a classic inverse quasi-static hysteresis model (Preisach [15][16], Jiles-Atherton [17][18] ...) extended to the dynamical effect via a first-order time derivation of the local induction field. This approach is particularly accurate as the physical nature of the simulated processes is well respected, however for

complex geometries, fine space discretization schemes are mandatory and this increases drastically the simulation times. Furthermore, the implicit nature of the material law creates convergence issues at saturation levels and under weak frequency conditions where dynamic effects are extremely limited. In this article, we propose an alternative solution to simulate simultaneously every magnetic loss contributions and to ensure convergence in every situation. Under a varying magnetic field excitation, macroscopic eddy currents generate through the cross section of the ferromagnetic sample. By increasing the velocity of this excitation, the eddy currents are rejected over the cross section peripheral areas according to the well-known electrical skin effect. These eddy currents behave as a magnetic shield preventing a complete magnetic field diffusion [19][20]. All these behaviors are analytically considered through the magnetic field diffusion equation derived from the Maxwell equations:

$$\nabla^2 H = \sigma \cdot \frac{dB}{dt} \quad (1)$$

In a ferromagnetic material, the magnetic diffusion and the related eddy currents interfere with the magnetic domain structure. These interactions distort the diffusion process and the classic diffusion equation is no more suitable to provide correct simulation results. This unusual diffusion process can be classified as anomalous and requires unfamiliar mathematic tools to be modeled. Such operators exist in the framework of fractional calculus, specifically fractional derivatives. By replacing the first-order magnetic induction field time derivation by a fractional one as proposed in (Eq. 2), flexibility is provided in the simulation scheme and very accurate simulation results can be obtained.

$$\nabla^2 H = \sigma \cdot \frac{d^\alpha B}{dt^\alpha} \quad (2)$$

By adjusting the fractional order of this modified diffusion equation, the obtained equation is able to simulate precisely all the dynamic magnetic losses contributions.

In the first part of this article, details will be provided as a reminder of the fractional derivative concept, then the modified diffusion equation and its resolution will be discussed. An experimental set-up will be described right after and comparisons simulations/measures used to validate our theory.

## II - Fractional derivative

Fractional derivatives generalize the concept of the derivative to non-integer orders. In applied mathematics and mathematical analysis, the fractional derivative is a derivative of any arbitrary order, real or complex [21]. A very limited number of functions can be analytically fractional derived. Trigonometric functions are some of them. Different definitions of fractional derivatives are available. The Grünwald-Letnikov [22] and the Riemann-Liouville [23][26] definitions are probably the most popular even if both of them are particular cases of a general fractional-order operator namely. The first one represents the  $\alpha$  order derivative, while the other represents the  $\alpha$  folds integral. The class of functions described by the Riemann-Liouville definition is broader (the function must be integrable) than the one defined by Grünwald and Letnikov. However, in the case of functions from the Grünwald-Letnikov class, both definitions are equivalent. It is important to keep in mind that fractional derivatives are rarely used in physics, they still generate lots of research efforts. According to Riemann and Liouville, the fractional derivative of a function  $f(t)$  is a convolution between  $f(t)$  and  $t^\alpha H(t)/\Gamma(1-\alpha)$  where  $\Gamma(\alpha)$  is the gamma function:

$$\frac{d^\alpha f(t)}{dt^\alpha} = D_t^\alpha f(t) = \frac{1}{\Gamma(1-\alpha)} \frac{d}{dt} \int_{-\infty}^t (t-\tau)^{-\alpha} f(\tau) d\tau \quad (3)$$

The additional time derivative present in the formula coincides with the occurrence of positive argument of the gamma function,  $\Gamma(\cdot)$ , leading towards its convergence to a finite value. From (Eq. 3), it is obvious that fractional derivatives include the memory of the previous states. Such property is fundamental while working with hysteretic behavior where current states depend strongly on the tested system or material history. From the spectral perspective, an interesting consequence of fractional derivatives is how the frequency spectrum  $f(\omega)$  is multiplied by  $(j\omega)^\alpha$  instead of  $j\omega$  for a first-order classic derivative.

In this study, after multiple tests, the Grünwald-Letnikov definition (Eq. 4) has been preferred as the convergence rate and the simulation times were noticed to be better.

$$\frac{d^\alpha f(t)}{dt^\alpha} = D_t^\alpha f(t) = \lim_{h \rightarrow 0} \frac{1}{h^\alpha} \sum_{k=0}^{\infty} (-1)^k \binom{\alpha}{k} f(t - kh) \quad (4)$$

$$\binom{\alpha}{k} = \frac{\alpha(\alpha-1)(\alpha-2)\dots(\alpha-k+1)}{\alpha!}$$

### III - Anomalous diffusion equation

#### III.1 - Introduction

Iron losses in a ferromagnetic material are related to both the macroscopic and the microscopic Eddy currents. The losses separation principle discretizes the losses contribution in 3 terms. In this article, the classical and the excess losses are jointly considered through a modified anomalous diffusion equation. In a ferromagnetic material, the domain wall distribution locally interferes with the magnetic field diffusion creating local interactions distorting the diffusion process which can be interpreted as an anomalous behavior. In physics, anomalous diffusion processes are frequent in complex media [27], anomalous diffusions are relatively commonly considered through fractional-order diffusion equation models [28][29]. Here, classically, the time derivative term is corresponding to a long-time heavy tail decay and the spatial derivative for diffusion nonlocality. Introducing fractional derivatives gives flexibility in the simulation process and it also leads to huge improvements in terms of accuracy [25][26][30]. In our particular case, the time derivative term is extended to a fractional order (Eq. 2). The Grünwald Letnikov fractional derivative definition is used to solve it:

$$\nabla^2 H = \sigma \cdot \lim_{h \rightarrow 0} \frac{1}{h^\alpha} \sum_{k=0}^{\infty} (-1)^k \binom{\alpha}{k} B(t - kh) \quad (5)$$

$B$  and  $H$  are connected through a sigmoid-type anhysteretic non-linear relation. This sigmoid function can be expressed from a Langevin-type function (Eq. 6):

$$\begin{cases} B_{an} = B_s \cdot \left[ \coth\left(\frac{H}{a}\right) - \frac{a}{H} \right] \\ \nabla^2 H = \sigma \cdot \lim_{h \rightarrow 0} \frac{1}{h^\alpha} \sum_{k=0}^{\infty} (-1)^k \cdot \binom{\alpha}{k} \cdot B_s \cdot \left[ \coth\left(\frac{H(t - kh)}{a}\right) - \frac{a}{H(t - kh)} \right] \end{cases} \quad (6)$$

Or from the Ising spin model (Eq. 7):

$$\begin{cases} B_{an} = B_s \cdot \tan^{-1}\left(\frac{H}{a}\right) \\ \nabla^2 H = \sigma \cdot \lim_{h \rightarrow 0} \frac{1}{h^\alpha} \sum_{k=0}^{\infty} (-1)^k \cdot \binom{\alpha}{k} \cdot B_s \cdot \tan^{-1}\left(\frac{H(t-kh)}{a}\right) \end{cases} \quad (7)$$

$B_s$  is the saturation induction,  $a$  is an intrinsic material parameter strongly dependent on the density of the domain walls.  $B_s$  and  $a$  are obtained by comparing simulation results to the experimental anhysteretic curve. Curve fitting toolbox from @Matlab software is used. Fig. 2 below, shows the comparison obtained after optimization for both the experimental and the simulated anhysteretic curve. It is worth mentioning that the experimental anhysteretic curve is an approximation as it has been reconstructed through average values from both increasing and decreasing branches of the experimental hysteresis cycle.

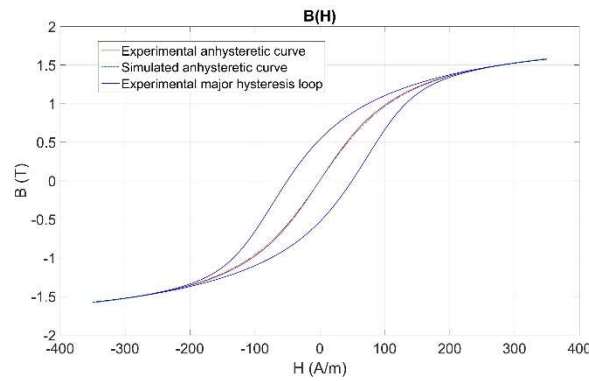


Fig. 2 – Comparison simulation/measure for the anhysteretic nonlinear behavior, ( $f = 1$  Hz, for the experimental conditions see part. V).

## II.2 - Resolution

The modified diffusion equation (Eq. 6) is solved through an Epstein frame-type cross section lamination. The geometrical and magnetic assumptions are those of the single sheet tester: unidirectional and homogeneous surface excitation field  $H$ , collinearity between  $B$  and  $H$ . We also assume the electrical conductivity  $\sigma$  as homogeneous and constant. Considering the dimensions of the studied lamination (width  $\gg$  thickness), a one-dimension (1-D) study in the thickness direction is carried out. The symmetry property of the single sheet tester allows to limit the study area to the half thickness of the lamination. The 1-D study limits the problem's variable number, (Eq. 8) becomes:

$$\begin{cases} B_{an} = B_s \cdot \tan^{-1}\left(\frac{H}{a}\right) \\ \frac{\partial^2 H}{\partial y^2} = \sigma \cdot \lim_{h \rightarrow 0} \frac{1}{h^\alpha} \sum_{k=0}^{\infty} (-1)^k \cdot \binom{\alpha}{k} \cdot B_s \cdot \tan^{-1}\left(\frac{H(t-kh)}{a}\right) \end{cases} \quad (8)$$

Taking into account the simplicity of the study domain, i.e. half thickness of a magnetic lamination, the finite differences method is used to solve (Eq. 9).

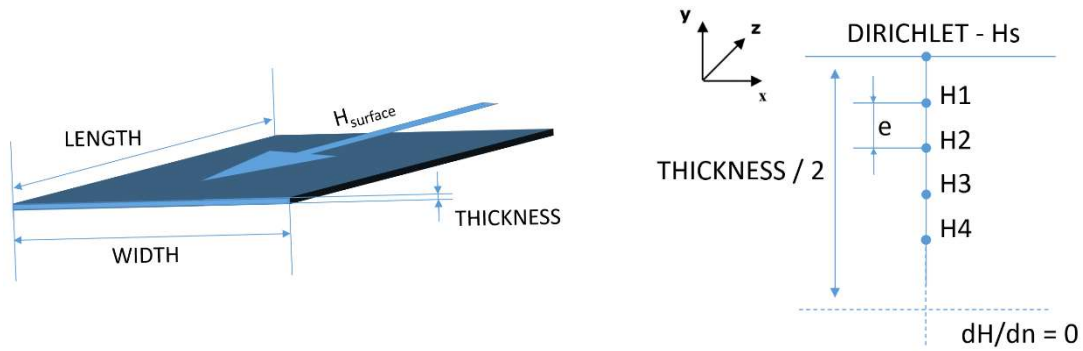


Fig. 3 – Simulation configuration.

Once every nodes' equation completed, a matrix system can be established:

$$[M] \cdot [X] = [S] \quad (9)$$

Where:

$$[M] = \begin{bmatrix} v_1 + 2 & -1 & . & . & . & 0 \\ -1 & v_2 + 2 & -1 & . & . & . \\ . & -1 & . & . & . & . \\ . & . & . & . & . & . \\ . & . & . & . & . & . \\ 0 & . & . & . & . & -2 \quad v_n + 2 \end{bmatrix}$$

$$v_i = \sigma \cdot \frac{B_s / a}{1 + \tan^2(B_i / B_s)} \cdot e^2 \cdot \left(\frac{1}{dt}\right)^\alpha$$

$$\left\{ \begin{array}{l} [S] = \begin{bmatrix} H_{\text{surface}} + \chi_1 \\ \chi_2 \\ \chi_3 \\ \vdots \\ \chi_n \end{bmatrix} \\ \chi_i = \sigma \cdot \frac{B_s / a}{1 + \tan^2(B_i / B_s)} \cdot e^2 \cdot \left( \frac{1}{dt} \right)^\alpha \sum_{k=0}^{t/dt} (-1)^k \cdot \binom{\alpha}{k} \cdot B_s \cdot \tan^{-1} \left( \frac{H_i(t - k \cdot dt)}{a} \right) \end{array} \right. \quad (10)$$

Here  $B_i$  and  $H_i$  are respectively the  $i$  node magnetic induction and excitation.  $e$  is the space step separating two differences nodes. For every time step, the matrix system is solved. Once all the  $B_i$  known, the material magnetic induction is calculated from direct average calculus:

$$B = \frac{\sum_1^n B_i}{n} \quad (6)$$

#### IV - Losses simulation

The magnetic losses are calculated from the hysteresis cycle area. For the first simulation results (Fig. 5 below), surface  $H$  sine waveforms are imposed, the maximum amplitude is set to 350 A/m and the frequencies tested range from 2 to 4096 Hz. 10 values of fractional orders are tested from 0.1 to 1. The magnetic losses are negligible under weak frequency, they increase up to a maximum value and decrease continuously until reaching a negligible level. It is worth noticing through these first simulation results that the lack of losses under low frequency levels is justified from the absence of the quasi-static contribution. The effect of the fractional derivative consideration in the fractional diffusion equation can be described as a stretching of the Losses vs frequency curve. By decreasing the fractional-order, we decrease the maximum value of the magnetic losses and shift the peak in the rightward direction. From a hysteresis cycle point of view, the effect of this fractional-order decrease can be observed by a slow but continuous lay down of the hysteresis cycle.

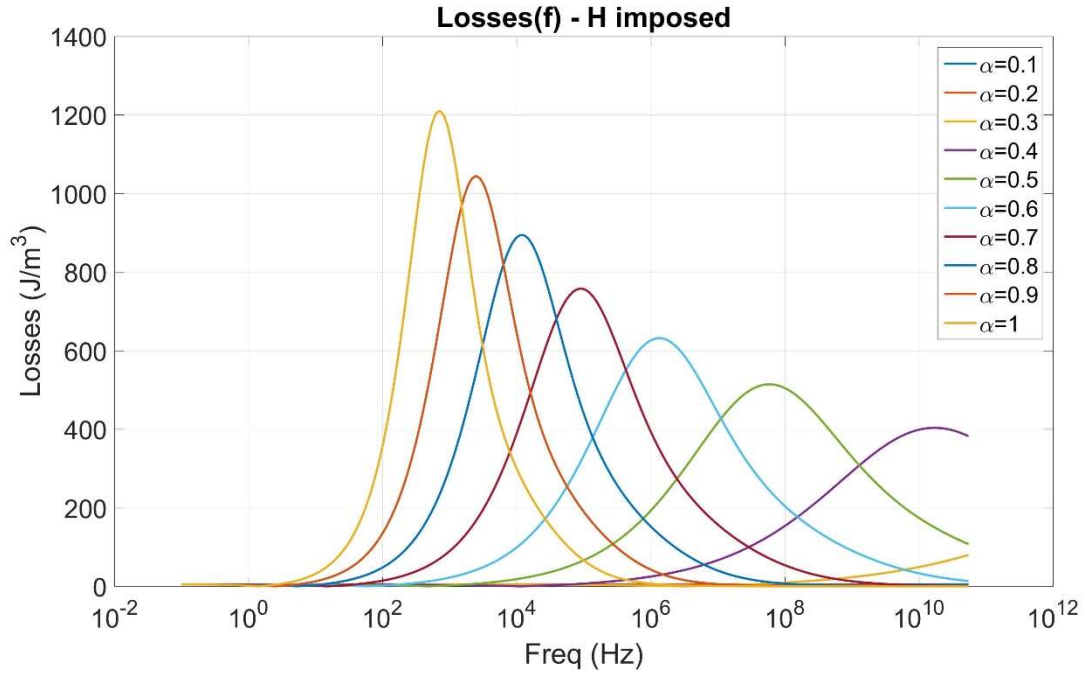


Fig. 5 – Hysteresis losses vs frequency for different values of  $\alpha$  (H imposed).

According to the ferromagnetic material characterization standards [31]-[33], to correctly characterize the hysteresis signature of a ferromagnetic material, the experimental tests have to be performed under “ $B$  imposed” sinus-type waveform. The anomalous diffusion equation (Eq. 5) can only be solved under “ $H$  imposed” conditions opposed to the standard conditions described in [31]-[33]. To address this issue, we used a feedback control and a proportional/integral corrector. This solution is described in Fig. 6. The corrector parameters are set from experimental optimization. Working under “ $B$  imposed” conditions is imposed by the norm but it is also a far much simpler way to consider the quasi-static contribution in our simulation. This quasi-static contribution can be provided from the usual quasi-static hysteresis models. The classic Preisach and Jiles-Atherton models in their inverse versions [34]-[36] can be by instance used with success for this contribution. To limit the size of this article, both these well-known models will not be described hereby but every details can be found in the literature [27][30]. After several tests, we selected the Jiles-Atherton model for its simplicity and its limited number of parameters.

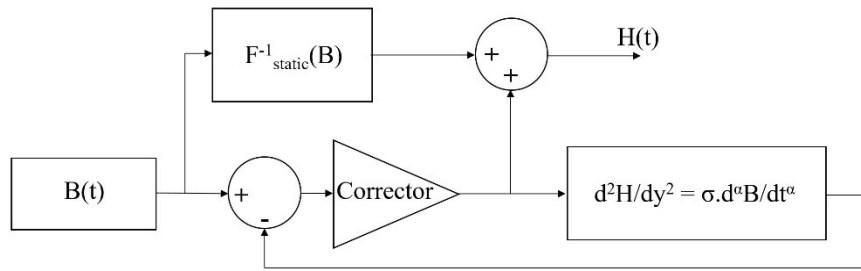


Fig. 6 – Hysteresis losses vs frequency for different values of  $\alpha$  (H imposed).

Fig. 7 shows the magnetic losses versus frequency simulation curves. The same 10 fractional orders are tested. 1.52T maximal amplitude is imposed. As illustrated in Fig.1, a continuous increasing is observed. The increasing rate depends on the fractional order.

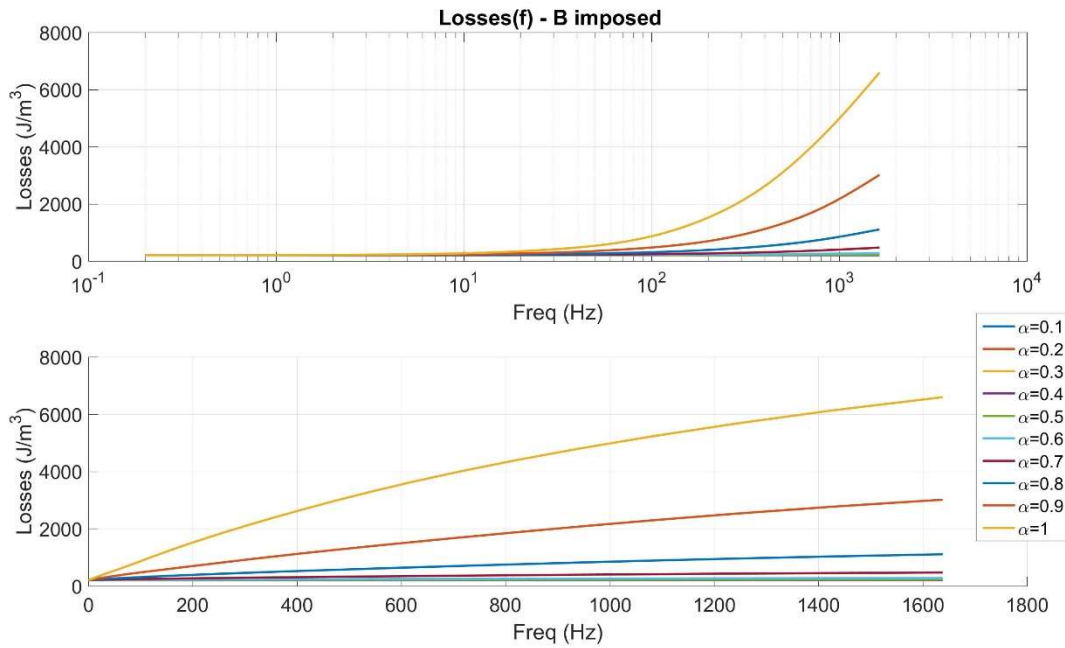


Fig. 7 – Hysteresis losses vs frequency for different values of  $\alpha$  (B imposed).

### V - Experimental set-up

In order to experimentally validate the theoretical concepts described in this article, comparisons simulations/measures have been performed. Magnetic lamination samples made out of a non-oriented SiFe material have been considered. These sheets are 3% silicon iron non-oriented grain electrical alloy referenced 35C330 grade. The manufacturer characteristics are given in Tab. I below.

Thickness in (mm)	PowerCore™ Grade	Magnetic Properties			Physical Properties			
		Core Loss W/kg at 1.0 T at 50Hz	Core Loss W/kg at 1.5 T at 50Hz	Magnetic Polarization (B) in Tesla at 5000 (A/m)	Vicker Hardness HV1	YS (N/mm <sup>2</sup> )	TS (N/mm <sup>2</sup> )	% EI at 80GL
0.35	35C330	1.25	3.15	1.63	180 +/- 15	295 +/- 30	445 +/- 30	Min 18

Tab. 1 – 35C330 properties from the manufacturer.

The tested specimens have Epstein frame dimensions: 280 mm long, 30 mm wide and a thickness of 0.35 mm. The conductivity is  $2.17 \cdot 10^6$  (S/m). Measurements have been performed using a single sheet tester according to the standard IEC 60404-3 [32]. Two coils of 200 turns each in series constitute the primary excitation. A double C-yoke, 300mm wide and made out of grain-oriented Fe-Si lamination leads the magnetic flow through the tested sample. A 100 turns surrounding sensor coil is used to measure the magnetic flux through the cross section of the magnetic sample. The schematic of the experimental set-up is shown in Fig. 8. Harmonic  $B$  imposed characterization is performed. Real time feedback control is ensured from a DEWESoftX2 data acquisition software associated with a SIRIUSif 8xCAN data acquisition and generation card. These devices ensure the control of the magnetizing current and the acquisition of the measured signals. The surface tangent excitation field  $H$  is monitored by a tesla-meter (Hall probe sensor). To ensure the reproducibility of our experimental conditions, the Hall Effect sensor is positioned in the middle and in contact with the ferromagnetic lamination, as close as possible of the sensor coil. A numerical integration is used to obtain the induction field variations from the surrounding coil sensor voltage measurements. A numerical correction is performed to get rid of the undesired drift due to the analogic integration. Before each new measure, we ensure the reproducibility of the result by a complete demagnetization of the tested samples. The same experimental setup is used for this operation; the excitation winding is subjected to a slowly decreasing amplitude, 50 Hz triangular voltage signal. This process ensures a fully demagnetization under controlled rate of flux variation. The magnetization process lasts less than 2 minutes.

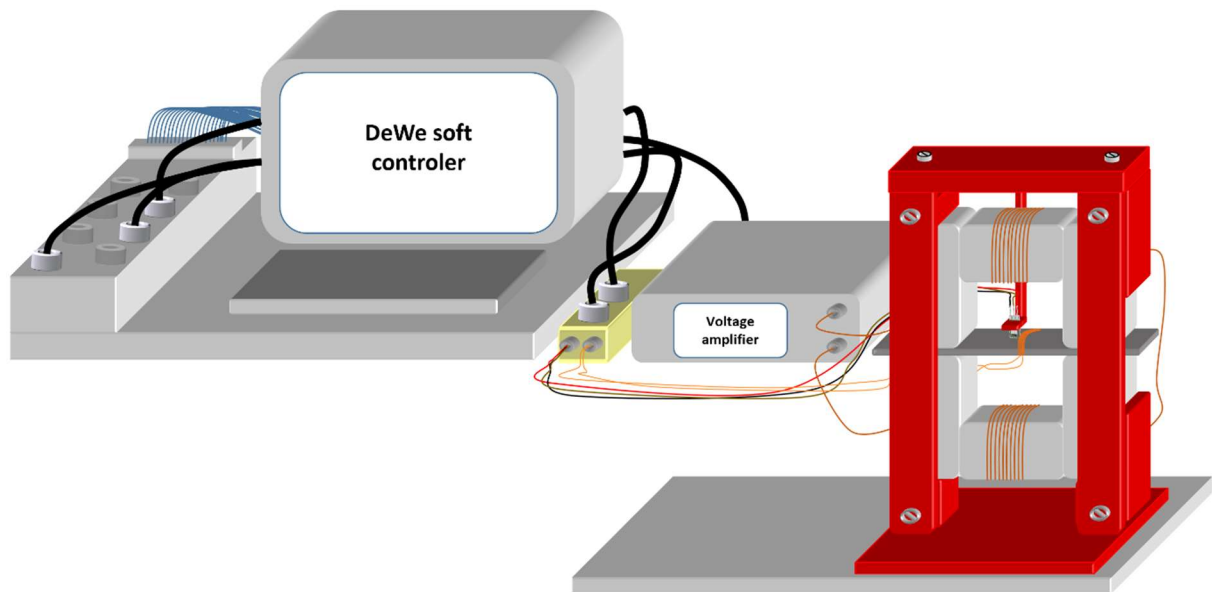


Fig. 8 – Experimental set-up, single sheet tester.

## VI - Comparison simulations/measures and validation of the simulation approach

Extensive experimental tests have been performed, the most significant being displayed hereafter. Fig. 9 gives a first illustration of the most accurate results obtained from the resolution of the anomalous diffusion equation. Comparison simulations/measures are displayed for 1.52 T “*B* imposed” sinus waveform with frequencies varying from 1 Hz to 400 Hz. Tab. 2 below gives the simulation parameters:

Simulation parameters			
$\sigma$ (S / m)	$B_s$ (T)	$a$	$\alpha$
2.22	1.2	0.01	0.91

Tab. 2 – Simulation parameters (Eq. 10).

The accuracy of the simulation approach is obvious. Best simulation results are obtained for a fractional order set to 0.91. This 0.91 fractional order can be physically interpreted as the best compromise between the first-order classical losses contribution and the square root order excess losses. The level of 1.52 T has been chosen as it ensures a complete magnetization state. Even if not displayed in this article, it is worth mentioning that results obtained from lower amplitude tests exhibit very similar accuracy. Fig. 10 shows a comparison between the simulation and the measure on the hysteresis losses vs frequency curve,  $\alpha = 0.91$  curve is the only one plotted here as it gives the best results. 5% error

bars have been added in the measured “Losses(*f*)” curve as it corresponds to the uncertainty of our experimental setup.

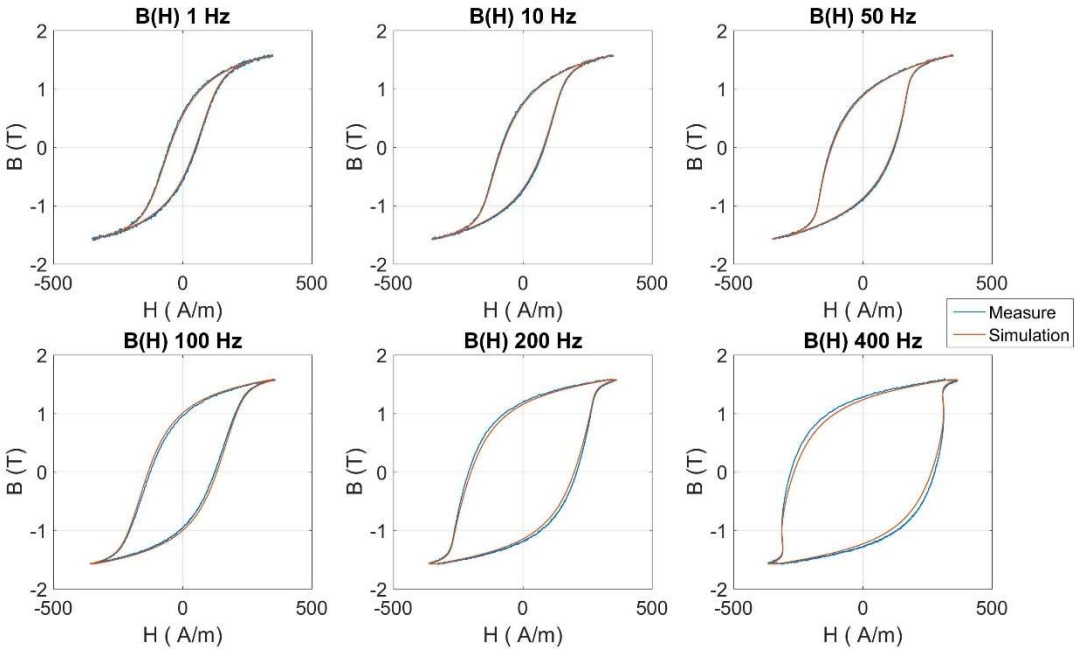


Fig. 9 – Comparisons simulations/measures for major hysteresis cycles under magnetic excitation of increasing frequencies (1 to 400 Hz).

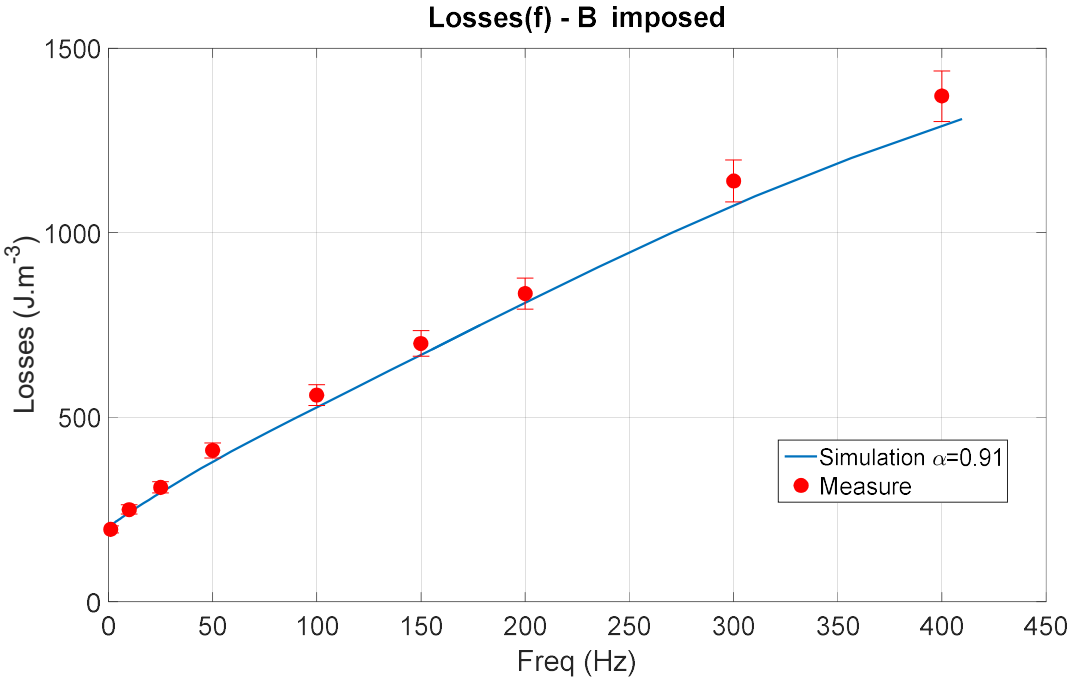


Fig. 10 – Comparison simulation/measure for the magnetic losses vs frequency curve.

An interesting aspect of the space discretization finite differences approach is the access to the sub-surfacic and the in-depth field distributions (*H<sub>i</sub>* and *B<sub>i</sub>*). In the last figure of this article, we show the

depth distribution of the magnetic state as a function of the frequency for different values of  $\alpha$ . The obtained results confirm several intuitive conclusions, i.e. a full magnetization state for weak  $\alpha$  values and even under very high frequency excitation. By opposition huge variations of the magnetic distribution vs frequency can be observed for high  $\alpha$  fractional orders. When  $\alpha = 1$  the transition state between full magnetization and no magnetization stands in a relatively narrow frequency bandwidth, by decreasing alpha the frequency bandwidth enlarges as an inverse proportion of the  $\alpha$  variations.

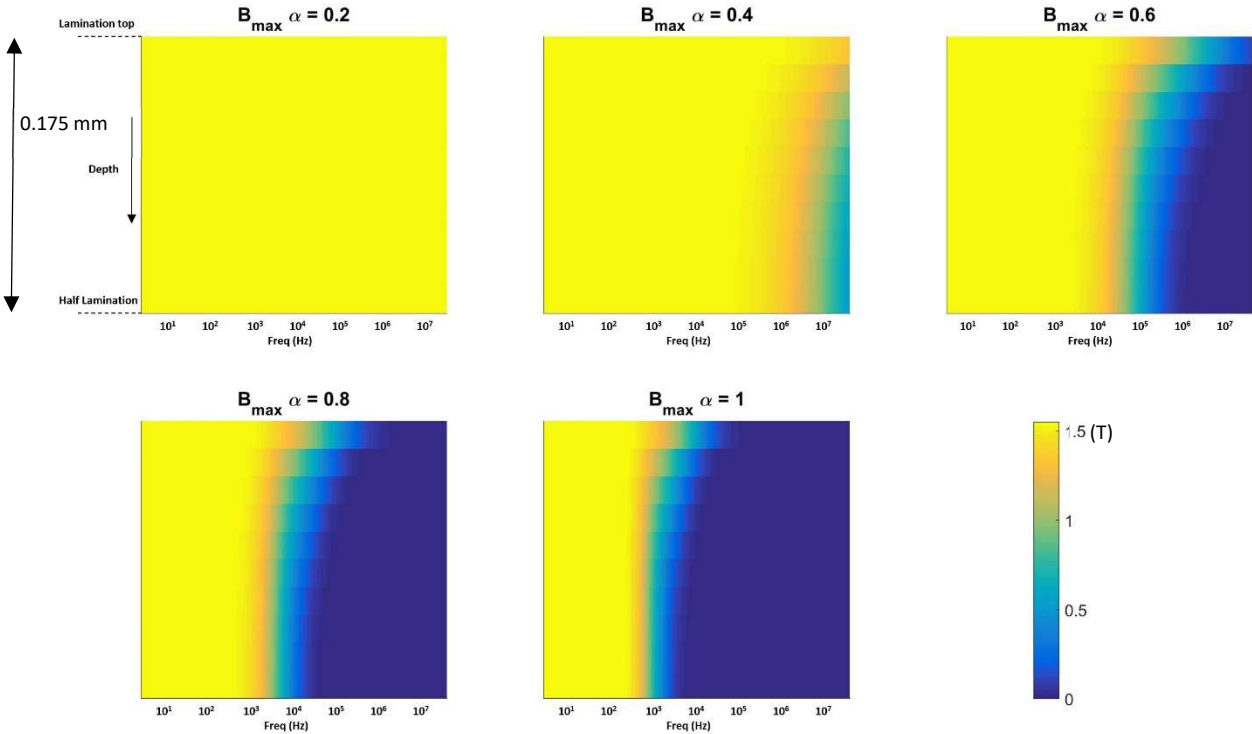


Fig. 11 – Hysteresis losses vs frequency for different values of  $\alpha$  (H imposed).

**VII - Conclusion**

Fractional diffusion equations have already been used with success to simulate anomalous diffusive behaviors. In this article, it is shown its effectiveness for the simulation of the magnetic field diffusion through a ferromagnetic material. The influence of the magnetic domains and their activities on the diffusion of the magnetic field is strong. They clearly disturb the process and the resulting diffusion can with no doubt be classified as anomalous. In this paper, we explain in details how the classic magnetic diffusion equation has been modified with fractional derivative operators and illustrate the strong

performances obtained with the new formulation thanks to accurate comparisons with experimental results. From the iron losses and hysteresis frequency dependence point of view, as the fractional order gives flexibility in the simulation scheme, by adjusting it, classical and excess losses can be simulated simultaneously and through a single term. Such approach can, in some way, be interpreted as a much more coherent reading of the physical situation where macroscopic and microscopic eddy currents are continuously interacting and can't hardly be separated. In this article, we have limited the simulation effort to a 1D geometrical situation, future work should extend these results on geometry where 2D and even 3D simulations are mandatory.

**Conflict of Interest:**

**Funding:**

\_ This study was funded by the SCAC (Service de cooperation et d'action culturelle) of the French Embassy to Cameroon.

\_ This study was funded by the National Natural Science Foundation of China (Grant N° 51805298) and by the Natural Science Foundation of Shandong Province (Grant No. ZR201807090390).

## References

- [1] G. Bertotti, "hysteresis in magnetism", academic press, Elsevier, 1987.
- [2] M. A. Raullet, B. Ducharne, J.P. Masson, and G. Bayada, "The magnetic field diffusion equation including dynamic hysteresis: a linear formulation of the problem", IEEE Trans. on Mag., vol. 40, n° 2, pp. 872-875, 2004.
- [3] V. Mazauric, M. Drouineau, L. Rondot, "Assessing anomalous losses with dynamic hysteresis model", Int. J. of App. Elect. and Mech., vol. 33, pp. 95-101, 2010.
- [4] S. Zirka, Y. Moroz, P. Marketos, A. Moses, "A viscous-type dynamic hysteresis model as a tool for separation in conducting ferromagnetic laminations", IEEE Trans. on Mag., vol. 41, iss. 3, pp. 1109-1111, 2005.
- [5] T. Chevalier, A. Kedous-Lebouc, B. Cornut, C.Cester, "A new dynamic hysteresis model for electrical steel sheet", Phys. B, vol. 275, pp. 197-201, 2000.
- [6] B. Zhang, B. Gupta, B. Ducharne, G. Sebald, T. Uchimoto, "Preisach's model extended with dynamic fractional derivation contribution", IEEE Trans. on. Mag, vol. 54, iss. 3, 2017.
- [7] B. Zhang, B. Gupta, B. Ducharne, G. Sebald, T. Uchimoto, "Dynamic magnetic scalar hysteresis lump model, based on Jiles-Atherton quasi-static hysteresis model extended with dynamic fractional derivative contribution", IEEE Trans. on. Mag, iss. 99, pp. 1-5, 2018.
- [8] F. Bitter, Phys. Rev., Vol. 38, pp. 1903, 1931.
- [9] P. Weiss, "L'hypothèse du champ moléculaire et la propriété ferromagnétique", J. de Phys., vol. 6, pp. 661, 1907.
- [10] P. Weiss, J. Phys. Theor. Appl., 6 (1) (1907), pp.661-690. [4] R.H. Pry, C.P. Bean, J. Appl. Phys., vol. 29 (1958), 532-533.
- [11] R.H. Pry, C.P. Bean, J. Appl. Phys., vol. 29, pp. 532-533, 1958.
- [12] Ch. P. Steinmetz, "On the law of hysteresis", reprint, Proc. IEEE, vol. 72, iss. 2, pp. 196-221, 1984.
- [13] G. Bertotti, "General Properties of Power Losses in Soft Ferromagnetic Materials", IEEE Trans. on Mag., vol. 24, iss. 1, pp. 621-630, 1980.
- [14] V. Basso, G. Bertotti, O. Bottauscio, F. Fiorillo, M. Pasquale, "Power losses in magnetic laminations with hysteresis: Finite element modeling and experimental validation", J. Appl. Phys., vol. 81, iss. 8, 1997.
- [15] F. Preisach, "Über die magnetische Nachwirkung", Zeitschrift für Physik, Bd. 94, 1935.
- [16] I.D. Mayergoyz, G. Friedman, "Generalized Preisach Model of Hysteresis", IEEE trans. on Mag., vol. 24, iss.1, pp. 212-217, 1988.
- [17] D.C Jiles, D.L Atherton, "Theory of ferromagnetic hysteresis", J. of Mag. and Mag. Mat., Vol. 61, pp. 48-60, 1986.

- [18] D. C. Jiles, "Modelling the Effects of Eddy Current Losses on Frequency Dependent Hysteresis in Electrically Conducting Media" IEEE Transactions On Magnetics, Vol.30, N°6, 1994.
- [19] B. Ducharne, G. Sebald, D. Guyomar, G. Litak, "Fractional model of magnetic field penetration into a toroidal soft ferromagnetic sample", Int. J. of Dyn. And Cont., pp. 1-8, 2017.
- [20] B. Ducharne, G. Sebald, D. Guyomar, G. Litak "Dynamics of magnetic field penetration into soft ferromagnets", Journal of Applied Physics, pp. 243907, 2015.
- [21] A.K. Grünwald, "Ueber begrenzte derivationen und deren Anwendung", Z. Math. Phys. XII, pp. 441-480, 1867.
- [22] B. Riemann, Gesammelte Werke, 1892.
- [23] J. Liouville, "Mémoire sur le calcul des différentielles à indices quelconques", J. Ecole Pol., Paris, vol. 13, pp. 71–162, 1983.
- [24] A. Atangana, A. Kilicman, "On the Generalized Mass Transport Equation to the Concept of Variable Fractional Derivative". Mathematical Problems in Engineering, vol. 9, 2014.
- [25] D. Guyomar, B. Ducharne, G. Sebald, "Time fractional derivatives for voltage creep in ferroelectric materials: theory and experiment", J. of Phys. D: App. Phys., Vol. 41, Iss. 12, 125410, 2008.
- [26] D. Guyomar, B. Ducharne, G. Sebald, "Dynamical hysteresis model of ferroelectric ceramics under electric field using fractional derivatives", Journal of Physics D: Applied Physics, vol. 40, Iss. 19, pp. 6048-6054, 2007.
- [27] R. Metzler, J. Klafter, "The random walk's guide to anomalous diffusion: a fractional dynamics approach". Phys. Rep., vol. 339, iss. 1, pp. 1-77, 2000.
- [28] F. Mainardi, Y. Luchko, G. Pagnini, "The fundamental solution of the space-time fractional diffusion equation", Fractional Calculus and Applied Analysis, vol. 4, iss. 2, pp. 153–192, 2001.
- [29] A. Atangana, D. Beleanu, "Fractional Diffusion Processes: Probability Distributions and Continuous Time Random Walk", Lecture Notes in Physics, vol. 621, p. 148, 2007.
- [30] J.M. Colbrook, X. Ma, F.P. Hopkins, J. Squire, "Scaling laws of passive-scalar diffusion in the interstellar medium". Monthly Notices of the Royal Astronomical Society, vol. 467, iss. 2, pp. 2421–2429, 2017.
- [31] IEC 60404-2, "Magnetic materials – Part 2: Methods of measurement of the magnetic properties of electrical steel strip and sheet by means of an Epstein frame", Int. Elect. Com., June 2008.
- [32] IEC 60404-3, "Magnetic materials – Part 3: Methods of measurement of the magnetic properties of electrical steel strip and sheet by means of a single sheet tester", Int. Elect. Com., April 2010.
- [33] IEC 60404-6, "Magnetic materials – Part 6: Methods of measurement of the magnetic properties of magnetically soft metallic and powder materials at frequencies in the range 20 Hz to 200 kHz by the use of ring specimens", Int. Elect. Com., June 2003.
- [34] J. V. Leite, N. Sadowski, P. Kuo-Peng, N. J. Batistela, and J. P. A. Bastos, "The inverse Jiles-Atherton model parameters identification," IEEE Trans. Magn., vol. 39, no. 3, pp. 1397–1400, 2003.

[35] J. V. Leite, N. Sadowski, P. Kuo-Peng, N. J. Batistela, J. P. A. Bastos, and A. A. de Espindola, "Inverse Jiles–Atherton vector hysteresis model," *IEEE Trans. Magn.*, vol. 40, no. 4, pp. 1769–1775, 2004.

[36] E. Cardelli, E.D. Torre, B. Tellini, "Direct and inverse Preisach modeling of soft materials", *IEEE Trans. on Mag.*, vol. 36, iss. 4, pp. 1267-1271, 2000.